



# Comparison of modeled ozone distributions with ozonesonde observations in the tropics

*Rob Puts*

**Scientific report = Wetenschappelijk Rapport; WR 2001-02**

De Bilt, 2001

PO Box 201  
3730 AE De Bilt  
Wilhelminalaan 10  
<http://www.knmi.nl>  
Telephone +31 30 220 69 11  
Telefax +31 30 221 04 07

Author: Rob Puts

UDC: 551.510.534  
551.501.71  
551.508.952

ISSN: 0169-1651

ISBN: 90-369-2191-0



# Comparison of modeled ozone distributions with ozonesonde observations in the tropics

*Rob Puts*



**Coaches:** dr. J. P. F. Fortuin  
dr. P. F. J. van Velthoven  
**Supervisor:** prof. dr. H. M. Kelder





## Abstract

Modelling as a tool for supporting research on major scientific questions in atmospheric chemistry and climate research, has received a lot of attention during the last decades. Many aspects of modelling atmospheric processes have been investigated.

In this report, the global three-dimensional chemistry transport model of the Royal Netherlands Meteorological Institute (KNMI), TM3, is used to compare ozonesonde profiles in the tropics with corresponding modeled ozone distributions in order to validate the model results for ozone. TM3 uses 6-hourly meteorological data from European Centre for Medium-Range Weather Forecasts (ECMWF)-analysis and includes parameterisations for subgrid scale processes such as convection. TM3 includes an ozone chemistry module containing the methane and carbon monoxide oxidation chain for the troposphere and lower stratosphere.

Our study was limited to three ozonesonde stations in the tropics: Ascension Island, Nairobi and San Cristobal. Generally, monthly mean modeled ozone profiles compare reasonably well for all three stations with the natural variability constructed from all the available observations in the corresponding months, except for the upper stratosphere (above 50 mbar). In the upper stratosphere, an evident systematic deviation is visible. From this, it can be concluded that the prescribed climatology for the upper stratosphere in TM3 is less reliable for the tropics, due to the low number of included observations in the tropics.

Furthermore, the seasonality of ozone for the ozonsonde stations Ascension Island and Nairobi has been investigated. For Ascension Island, which is located on an island far away from the continents and therefore should not be affected by local pollution, the seasonality is reproduced quite well by TM3, except for – again – the upper stratosphere. For Nairobi, which is located at the equatorial East-coast of Afrika, the seasonality is only reproduced reasonably well in the lower troposphere.

Finally, an attempt has been made to investigate the possibility to reproduce daily changes in ozone profiles with TM3. For this, individual soundings in September 1998 at the San Cristobal station were simulated. The conclusion is that the modeled ozone profiles are not accurate or sensitive enough to show detailed features. Probably this can be explained by the very high spatial and temporal resolution required to reproduce these fine structures. The used model resolution of  $8^\circ \times 10^\circ \times 19$  vertical layers is probably not fine enough.

*Key words index:* TM3, ozone, tropics.



# Contents

<b>1</b>	<b>INTRODUCTION.....</b>	<b>1</b>
<b>2</b>	<b>MODEL DESCRIPTION.....</b>	<b>2</b>
2.1	<i>Model resolution .....</i>	<i>2</i>
2.2	<i>Transport .....</i>	<i>4</i>
2.3	<i>Chemistry.....</i>	<i>5</i>
2.4	<i>Main chemical reaction mechanism .....</i>	<i>9</i>
<b>3</b>	<b>COMPARISON OF OZONE PROFILES .....</b>	<b>11</b>
3.1	<i>Scope of investigation .....</i>	<i>11</i>
3.2	<i>Ascension Island.....</i>	<i>13</i>
3.3	<i>Nairobi.....</i>	<i>15</i>
3.4	<i>San Cristobal.....</i>	<i>17</i>
<b>4</b>	<b>CONCLUSIONS .....</b>	<b>19</b>
<b>5</b>	<b>EPILOGUE AND ACKNOWLEDGEMENTS .....</b>	<b>20</b>
<b>6</b>	<b>REFERENCES.....</b>	<b>21</b>
	<b>APPENDIX A .....</b>	<b>23</b>
	<b>APPENDIX B .....</b>	<b>26</b>
	<b>APPENDIX C .....</b>	<b>28</b>
	<b>APPENDIX D.....</b>	<b>31</b>





# 1 Introduction

Models merely provide a limited, simplified description of reality. However, models can help to gain insight into relevant processes in the real atmosphere. Therefore, models are important tools for research on major scientific questions in atmospheric chemistry and climate research. Validation of such models is essential in order to assure the quality of the impact studies. This can be done by comparing the modeled with observed ozone distributions.

In this paper, the global three-dimensional chemistry transport model of the Royal Netherlands Meteorological Institute (KNMI), TM3, is used to compare observed ozonesonde profiles in tropics with corresponding modeled ozone distributions in order to validate the model results for ozone.

The contents of this paper are as follows. A model description of the TM3 model is given in chapter 2. Chapter 3 gives a detailed comparison of modeled and observed ozone profiles using available ozonesonde data for various stations in the tropics. Differences for individual stations as well as systematic discrepancies are identified. It also discusses several explanations for the discrepancies between the modeled and observed ozone distributions. Finally, chapter 4 gives some main conclusions.

## 2 Model description

The three-dimensional chemical transport model of the KNMI (TM3) has been adapted from the global tracer transport model TM2 [cf. Heimann, 1995]. TM3 calculates the horizontal and vertical transport of tracer mass on the basis of six hourly output from the European Centre for Medium-range Weather Forecasts (ECMWF) model [cf. Meijer, 2000]. The analyzed meteorological fields of wind, surface pressure, geopotential height, temperature, clouds and humidity with a horizontal resolution of  $2.5^\circ \times 2.5^\circ$  are used for this purpose. These meteorological data contribute to a rather realistic description of the actual meteorological situation since observations are included in the ECMWF analyses. The meteorological data are preprocessed for use in TM3. This involves the evaluation of parameterisations of subgrid scale processes and the integration/interpolation of data to the model grid of TM3.

### 2.1 Model resolution

For the present study TM3 was run with a horizontal resolution of  $10^\circ$  in longitude and about  $8^\circ$  in latitude. The longitudes ( $\lambda_i$ ) and latitudes ( $\beta_i$ ) of the centres of the grid boxes are located at

$$\lambda_i = -180^\circ + \frac{360^\circ(i-1)}{im} \quad (2.1.1)$$

and

$$\beta_i = -90^\circ + \frac{180^\circ(j-1)}{jm} \quad (2.1.2)$$

where  $i=1,2,3,\dots,im$  with  $im=36$  the number of boxes in the zonal and  $j=1,2,3,\dots,jm$  with  $jm=24$  the number of boxes in meridional direction. Here, longitudes West of Greenwich and latitudes in the southern hemisphere are denoted by negative values of  $\lambda$  and  $\beta$ , respectively. The boundaries of the grid boxes are situated halfway between two neighbouring centers. There is only one grid box centered on each of the Poles (namely  $i=1$  for  $j=1$  and  $j=jm$ ) and these polar grid boxes have a meridional extent of  $\frac{90^\circ}{jm}$  i.e. half the meridional extent of the grid boxes at other latitudes. The horizontal grid is illustrated in Fig. 2.1.1.

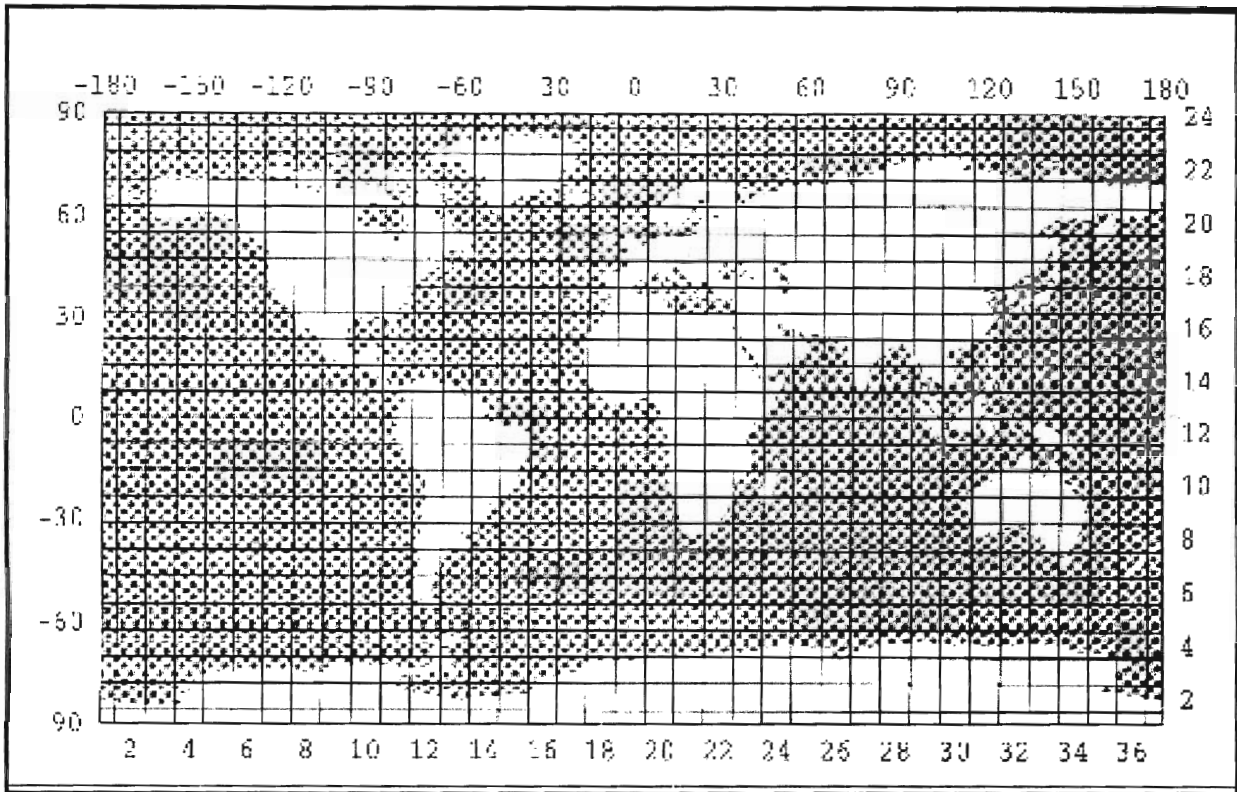


Figure 2.1.1 Illustration of the horizontal grid taken from Heimann [1995]. The numbers on the top and left border denote longitude and latitude in degrees, whereas the numbers on the bottom and right border are the longitudinal ( $i$ ) and latitudinal ( $j$ ) indices of the gridboxes.

Vertically, the model has 19  $\sigma$ -levels. The lower boundary of this coordinate system coincides with the surface whereas its upper boundary is situated at 0 hPa. The pressure  $p_k$  of the  $k$ -th  $\sigma$ -level can be obtained from

$$p_k = \sigma_k (p_s - p_t) \quad (2.1.3)$$

where  $p_s$  is the surface pressure and  $p_t$  is the pressure at the upper boundary of the model. The surface pressure depends on the location and varies in time. The main part of the spatial variation is due to differences in the elevation of the surface. High surface pressure values occur over the oceans whereas low values are located over elevated areas such as the Himalayas and the Antarctic.

## 2.2 Transport

The advection of tracers in TM3 is calculated with the slopes scheme of Russell & Lerner [1981]. The amount of tracers in each grid box is specified by its mass and the slopes of tracer mass in the zonal, meridional and vertical direction. The mass fluxes through each boundary of the grid box are computed from the ECMWF analyses in the pre-processing stage and stored for use in TM3. The amount of tracer mass transported in a time step from one cell to another can then be calculated. This can be used to calculate the new tracer mass in a grid box and its slopes. If the gradients in the spatial distribution of tracer mass are strong, the slope might be such that a negative value of the tracer mass occurs at the boundary of a grid box. This may lead to advection of negative tracer mass and even to negative values for the total tracer mass in a grid box. Since this is not realistic and can lead to problems in the chemistry module, the slopes are limited such that no negative tracer masses occur at the boundaries of the grid boxes. The advection time step used for the computations on the  $8^\circ \times 10^\circ$  horizontal grid of TM3 is one hour. One such model time step is a combination of 4 advection time steps in the East-West, 2 in North-South and 1 in the vertical direction. Afterwards vertical adjustment is applied in order to conserve mass.

In addition to vertical advection subgrid scale vertical transport occurs. This sub scale transport is obtained from parameterisations for cumulus and shallow convection and vertical diffusion. The vertical transport associated with these processes is also determined from ECMWF analyses data in the pre-processing stage.

The subscale convection fluxes are evaluated according to the scheme of Tiedtke [1989]. This scheme uses the water vapour convergence in combination with the evaporation from the surface in order to detect the presence of a cloud. In case a cloud is present a convection matrix is constructed which gives the fraction of tracer mass from one grid box that ends up in another due to the convection process. Here the altitude at which surface air condensates when lifted adiabatically gives the cloud base height and the altitude at which the cloud parcel is no longer buoyant defines its top. The air mass flux remaining at the top of the cloud is detrained in the two layers above the cloud top to simulate overshooting.

The vertical diffusion is calculated based on the stability of air using the formulation of Louis [1979]. This scheme, which utilises a stability function involving the Richardson number, yields the largest diffusion coefficients in the boundary layer.

## 2.3 Chemistry

TM3 contains a chemistry module from the MOGUNTIA model [cf. Crutzen & Zimmermann, 1991]. This scheme evaluates the time evolution of 13 trace gases according to the so-called quasi steady state assumption. This means that the chemical production and loss terms, denoted by  $P$  and  $L$  respectively, are assumed to be constant during the chemical time step  $\Delta t$ . The time evolution of the concentration of a trace gas  $C$  is then given by

$$\frac{dC}{dt} = P - LC \quad (2.3.1)$$

Note that the changes in the concentration of a trace gas due to advection and convection are not included in the above relation. These processes are considered in other modules of TM3. The solution of the differential equation (2.3.1) is

$$C_{t+\Delta t} = \left( C_t - \frac{P}{L} \right) \exp(-L\Delta t) + \frac{P}{L} \quad (2.3.2)$$

which is a relatively computer demanding expression to evaluate. For trace gasses with a relatively short lifetime ( $L^{-1} \ll 1$ ) this expression can be approximated by the so-called steady state solution (i.e.  $\frac{dC}{dt} = 0$ )

$$C_{t+\Delta t} = \frac{P}{L} \quad (2.3.3)$$

On the other hand, an expansion of the exponential factor in Taylor series yields

$$C_{t+\Delta t} = C_t + (P - LC_t)\Delta t, \quad (2.3.4)$$

which can be used for trace gases with a relatively long lifetime. This last solution is called explicit because the concentration on the right hand side of the differential equation is evaluated at time  $t$ . Sometimes this technique leads to stability problems resulting in the occurrence of negative concentrations. This implicit technique, which uses the concentration at  $t + \Delta t$ , gives for trace gases with a relatively long lifetime

$$C_{t+\Delta t} = \frac{P\Delta t + C_t}{1 + L\Delta t} \quad (2.3.5)$$

which is always stable. One of these above mentioned solutions for the differential equation (2.3.1) describing the time evolution of a trace gas is used for each trace gas, depending on its lifetime. The gases with relatively long lifetimes, i.e.  $O_3$ ,  $NO_x$ ,  $H_2O_2$ ,  $CH_4$ ,  $CO$ ,  $HNO_3$  and  $CH_3OOH$ , are transported in TM3, where after their change due to chemistry is computed. The concentrations of the trace gases with relatively short lifetimes, i.e.  $HCHO$ ,  $NO$ ,  $HO_2$ ,  $CH_3O_2$ ,  $O(^1D)$  and  $OH$ , are calculated in the chemistry module by the assumption of steady state.

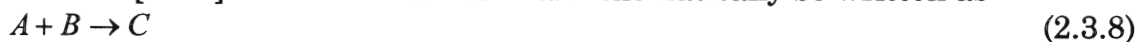
During daytime the chemical module contains 7 photo-dissociation reactions and 18 thermal reactions (cf. Table 2.3.1). Photo-dissociation is a chemical reaction in which a molecule absorbs a quantum of radiation  $h\nu$  and dissociates. This can be written schematically as



with A, B and C concentrations of trace gases. The reaction rate of photodissociation reaction is given by

$$\frac{dB}{dt} = Aj \quad (2.3.7)$$

with  $j$  the photolysis rate of the reaction. In the chemical module daytime averaged photolysis rates for O<sub>3</sub>, NO<sub>2</sub>, H<sub>2</sub>O<sub>2</sub>, HNO<sub>3</sub>, CH<sub>3</sub>COOH and HCHO are used, which have been computed off-line with the model described in Bruhl & Crutzen [1989]. Thermal reactions can schematically be written as



and proceed at the rate

$$\frac{dC}{dt} = kAB \quad (2.3.9)$$

with  $k$  the rate coefficient of the reaction. Expressions for the rate coefficients are taken from De More et al. [1992] and Atkinson et al. [1992] and are listed in Table 2.3.1. These reaction rates are calculated by using the pressure, temperature and relative humidity fields from the ECMWF analyses. During nighttime the chemistry module evaluates an off-line parameterised heterogeneous reaction. This parameterisation, which is based on the work of Dentener & Crutzen [1993], converts NO<sub>2</sub> and O<sub>3</sub> into HNO<sub>3</sub> and accounts for the heterogeneous conversion of N<sub>2</sub>O<sub>5</sub> into HNO<sub>3</sub>.

Additional sinks of trace gases are dry deposition of O<sub>3</sub>, NO<sub>2</sub>, H<sub>2</sub>O<sub>2</sub>, HNO<sub>3</sub>, CH<sub>3</sub>OOH and NO, and wet deposition of H<sub>2</sub>O<sub>2</sub>, HNO<sub>3</sub> and CH<sub>3</sub>OOH. The dry deposition flux  $F$  of a species is defined as the product of its concentration  $C$  (at a certain height above ground, which in the model is the centre of the lowest layer) and its dry velocity  $v$ ,

$$F = v.C \quad (2.3.10)$$

Constant deposition velocities are used for each of the tracers involved with distinctions between land and sea surface [cf. Hein, 1994]. According to Junge and Gustafsen [1957], wet deposition changes the concentration of a species according to

$$\frac{\partial C}{\partial t} = L_k.C \quad (2.3.11)$$

with the deposition rate  $L_k$  [s<sup>-1</sup>] given by

$$L_k = \frac{\varepsilon.P}{\Delta z_k.L} \quad (2.3.12)$$

$\varepsilon$  denotes the scavenging efficiency,  $P$  the precipitation rate which originates from the corresponding layer [mm/day] calculated from ECMWF's daily precipitation forecasts and a vertical distribution is given by climatology data from Newell et al. [1974],  $\Delta z_k$  the thickness of the model layer [m],  $L$  the volume fraction of liquid water in clouds.

Emissions of trace gases and/or surface mixing ratios of trace gases can be prescribed in the chemistry module. In general, the geographical and temporal distribution of emissions is pre-calculated and read from data files, whereas the absolute amount of global annual emissions is given as a parameter in the model code. Since the surface emissions for CH<sub>4</sub> and CO are not well established,

surface mixing ratios rather than emissions are specified. For this purpose prescribed surface concentrations have been used for CH<sub>4</sub> and CO according to Fung et al. [1991] and Dianov-Klokov & Yurganov [1981], respectively. NO<sub>x</sub> emissions are partitioned according to three source categories, namely NO<sub>x</sub> from aircraft traffic [Gardner et al., 1997], from lightning [Price and Rind [1992] and from several surface contributions.

Since the chemical scheme cannot adequately describe stratospheric chemistry, a zonally and monthly mean ozone climatology based on ozonesonde measurements [Fortuin and Langematz, 1995] is prescribed above 50 hPa. It should be noted that the quality of these climatological upper tropospheric ozone data is inhomogeneous due to the irregular spatial distribution of stations at which ozonesonde measurements take place. In particular, the data for the equatorial region and for the southern mid-latitudes are only based on few measurements and thus potentially less reliable than northern hemispheric data.

Also the destruction of CH<sub>4</sub> in the stratosphere through reactions with O(<sup>1</sup>D) and Cl is prescribed from monthly mean rates (calculated with a 2-dimensional stratosphere model [Bruhl & Crutzen, 1993]).

Table 2.3.1 The chemical reactions considered in TM3 during daytime and expressions for their reaction rates. Here n, T, p and H<sub>2</sub>O denote the density, temperature, pressure and water vapour concentration of the air in a grid box.

Code	Reaction	Rates
J1	$O_3 + hv \rightarrow O(^1D) + O_2$	
J2	$H_2O_2 + hv \rightarrow 2OH$	
J3	$NO_2 + O_2 + hv \rightarrow NO + O_3$	
J4	$HNO_3 + hv \rightarrow NO_2 + OH$	
J5	$HCHO + hv \rightarrow H_2 + CO$	
J6	$HCHO + 2O_2 + hv \rightarrow 2HO_2 + CO$	
J7	$CH_3OOH + O_2 + hv \rightarrow HCHO + HO_2 + OH$	
R1	$O(^1D) + O_2 + M \rightarrow O_3 + M$	KR1
R2	$O(^1D) + H_2O \rightarrow 2OH$	$2.2 \times 10^{-10}$
R3	$HO_2 + OH \rightarrow H_2O + O_2$	$4.8 \times 10^{-11} \exp(250/T)$
R4	$H_2O_2 + OH \rightarrow HO_2 + H_2O$	$2.9 \times 10^{-12} \exp(-160/T)$
R5	$O_3 + OH \rightarrow HO_2 + O_2$	$1.6 \times 10^{-12} \exp(-940/T)$
R6	$HO_2 + HO_2 \rightarrow H_2O_2 + O_2$	$(kR6a+kR6b)kR6c$
R7	$O_3 + HO_2 \rightarrow OH + 2O_2$	$1.1 \times 10^{-14} \exp(-500/T)$
R8	$HNO_3 + OH + O_2 \rightarrow NO_2 + O_3 + H_2O$	$KR8a + kR8c/(1+kR8c/kR8b)$
R9	$NO_2 + OH + M \rightarrow HNO_3 + M$	kR9
R10	$NO + HO_2 \rightarrow NO_2 + OH$	$3.7 \times 10^{-12} \exp(250/T)$
R11	$NO + O_3 \rightarrow NO_2 + O_2$	$2.0 \times 10^{-12} \exp(-1400/T)$
R12	$CH_4 + OH + O_2 + M \rightarrow CH_3O_2 + H_2O + M$	$2.9 \times 10^{-12} \exp(1820/T)$
R13	$CO + OH + O_2 \rightarrow CO_2 + HO_2$	$1.5 \times 10^{-13} (1+0.6p/1013.25)$
R14	$HCHO + OH + O_2 \rightarrow HO_2 + H_2O + CO$	$1.0 \times 10^{-11}$
R15	$CH_3O_2 + HO_2 \rightarrow CH_3OOH + O_2$	$3.8 \times 10^{-13} \exp(800/T)$
R16	$CH_3OOH + OH \rightarrow CH_3O_2 + H_2O$	$0.3 \times 3.8 \times 10^{-12} \exp(200/T)$
R17	$CH_3OOH + OH \rightarrow HCHO + OH + H_2O$	$0.7 \times 3.8 \times 10^{-12} \exp(200/T)$
R18	$CH_3O_2 + NO + O_2 \rightarrow HCHO + HO_2 + NO_2$	$4.2 \times 10^{-12} \exp(180/T)$

$$kR1 = [1.4058 \times 10^{-11} \exp(110/T) + 6.704 \times 10^{-12} \exp(70/T)]n$$

$$kR9 = kR9i / (1+kR9i/kR9h) 0.6^{**}(1 / (1 + (\log(R9i/kR9h))^2)) ; \text{ where}$$

$$kR9i = 2.6 \times 10^{-30} (T/300)^{-3.2} n \text{ and}$$

$$kR9h = 2.4 \times 10^{-11} (T/300)^{-1.3}$$

$$kR6a = 2.3 \times 10^{-13} \exp(600/T)$$

$$kR6b = 1.7 \times 10^{-33} \exp(1000/T) n$$

$$kR6c = 1.0 + 1.4 \times 10^{-21} \exp(2200/T) H_2O$$

$$kR8a = 7.2 \times 10^{-15} \exp(785/T)$$

$$kR8b = 4.1 \times 10^{-16} \exp(1440/T)$$

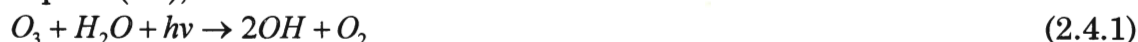
$$kR8c = 1.9 \times 10^{-33} \exp(725/T) n$$



## 2.4 Main chemical reaction mechanism

In this section the main chemical reaction mechanisms will be described. This description explains the oxidation of CH<sub>4</sub> via HCHO and CO into CO<sub>2</sub> by OH, the influence of NO<sub>x</sub> on the various paths that can be followed in this oxidation chain, and the resulting effect for O<sub>3</sub>. The chemical scheme continuously converts CH<sub>4</sub> and NO<sub>x</sub> via several intermediary products, which contains all kinds of feedback reactions, into CO<sub>2</sub> and HNO<sub>3</sub>, respectively. Emissions of CH<sub>4</sub> and NO<sub>x</sub> therefore end up as CO<sub>2</sub>, which is not chemically active, and HNO<sub>3</sub>, which is removed from the atmosphere by deposition. These chemical mechanisms influence the concentration of O<sub>3</sub> and that of other trace gases. The O<sub>3</sub> production and destruction by chemical reactions in the troposphere is more than the stratospheric input of O<sub>3</sub> in the troposphere. A more detailed description, involving all the reactions that are listed in table 2.3.1 and more, can be found in e.g. Dentener [1993], Crutzen [1995] and AERONOX [1995]. Here, only a brief overview will be given.

OH plays an important role in the oxidation of the most trace gases. The primary source of OH is photo-dissociation of O<sub>3</sub> (J1) followed by reaction with water vapour (R2), i.e.



The oxidation of CH<sub>4</sub> by OH gives CH<sub>3</sub>O<sub>2</sub> (R12). In NO-rich air this CH<sub>3</sub>O<sub>2</sub> oxidises to HCHO (R18). In NO-poor regions it leads to CH<sub>3</sub>OOH (R15), which oxidises to HCHO (R17, J7). HO<sub>2</sub> and CH<sub>3</sub>O<sub>2</sub> are products of the oxidation of CH<sub>4</sub>, which form NO<sub>2</sub> when being combined with NO (R10, R18). Photolysis of NO<sub>2</sub> leads to O<sub>3</sub> production in the troposphere and returns the NO again (J3). The net reaction in the NO<sub>x</sub> catalysed oxidation of CH<sub>4</sub> is, e.g. (R12+R18+R10+2J3)



Note that HO<sub>2</sub> and NO can also lead to the destruction of O<sub>3</sub> (R7, R11). The HCHO, which is produced in the oxidation of methane, is eventually transformed into CO (J6, J7, R14). The net oxidation of HCHO to CO is, e.g. (J6+2R10+2J3)



Oxidation of CO into CO<sub>2</sub> occurs via (R13). The net change due to oxidation of CO is either (R13+R10+J3)



or (R13+R7)

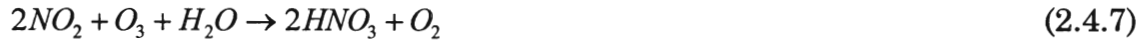


Hence, the oxidation of CO may lead to ozone production as well as destruction. In the presence of sufficient NO<sub>x</sub> reaction (R10) will dominate reaction (R7), so that the oxidation of CO leads to ozone production. In general, net chemical production of O<sub>3</sub> occurs in the NO<sub>x</sub>-rich and destruction in the NO<sub>x</sub>-poor regions of the troposphere.

The ratio between NO and NO<sub>2</sub> is mainly determined by the reaction of NO with O<sub>3</sub> that produces NO<sub>2</sub> (R11) and photolysis of NO<sub>2</sub> that converts it into NO again (J3). These reactions are so fast that a steady state is reached where

$$\frac{NO_2}{NO} = \frac{k_{11}}{j_3} O_3 \quad (2.4.6)$$

with  $k_{11}$  the rate coefficient of (R11) and  $j_3$  the photolysis rate of (J3).  $NO_2$  can be converted to  $HNO_3$  (R9), which is efficiently removed by dry and wet deposition. The above mechanisms are driven by photolysis and occur during daytime. At night the main sources of  $O(^1D)$ ,  $OH$  and  $NO$  are absent, so that these concentrations rapidly diminish. The only reaction that is considered in TM3 is then the heterogeneous reaction



### 3 Comparison of Ozone Profiles

#### 3.1 Scope of investigation

In this section, modeled ozone profiles of the global three-dimensional chemistry transport model of the KNMI (TM3) are compared with ozonesonde observations in the tropics in order to validate the model results for ozone. For that purpose, TM3 has been run for a period of two years using realistic tracer fields as start values derived from the output of a multiple-year run of the TM3 model. The first year was used to initialise the model. The results of the second year, obtained with the meteorological data from 1998, are analysed here.

In order to get a detailed validation of modeled ozone profiles, the modeled ozone profiles are compared with ozonesonde profiles at individual stations. In the initial stage of this study, the intention was to validate observations of the Paramaribo ozonesonde station. Unfortunately, no observations were available for the investigated year 1998. However, observations from a small number of stations operating in the southern hemisphere tropics and subtropics are available. But, these stations have a different launch frequency and different reporting procedures. SHADOZ [Southern Hemisphere Additional Ozonesondes] has been designed to remedy this data discrepancy by coordinating launches, supplying additional sondes in some cases, and by providing a central archive location. Data have been collected in a timely manner and have been made available through the SHADOZ website [Thompson and Witte, 1999] to the scientific community.

Table 3.1.1 lists the stations considered in the present comparison. It reports the geographical position of the stations together with the number of soundings in each month of 1998. Also the total number of soundings launched in 1998 is listed for each individual station. It can be seen that the soundings have been launched with a quite variable launch frequency.

Table 3.1.1 Ozonesonde stations used in the present comparison of modeled ozone profiles with observations.

Station	Latitude	Longitude	Number of soundings, 1998												Total
			January	February	March	April	May	June	July	August	September	October	November	December	
San Cristobal	0,92° S	89,6° E	-	-	4	2	-	-	-	-	7	2	2	2	20
Nairobi	1,27° S	36,8° W	4	4	4	5	4	3	-	-	4	5	4	4	41
Natal	5,42° S	35,38° E	1	-	2	1	-	-	-	-	-	-	1	-	5
Watakosek, Java	7,50° S	112,6° E	2	2	2	2	2	2	2	1	3	1	2	1	22
Ascension	7,98° S	14,42° W	8	5	7	-	7	6	5	7	4	5	8	6	68

Is.															
Am. Samoa	14,23 <sup>0</sup> S	170,56 <sup>0</sup> W	3	4	3	3	5	4	3	-	2	4	4	2	37
Tahiti	18,00 <sup>0</sup> S	149,00 <sup>0</sup> W	1	2	1	-	5	3	4	1	3	4	2	-	26
Fiji	18,13 <sup>0</sup> S	178,40 <sup>0</sup> E	4	4	2	6	3	3	3	1	4	2	3	4	39
La Reunion	21,06 <sup>0</sup> S	55,48 <sup>0</sup> E	2	1	-	2	1	1	2	1	2	2	2	2	18
Irene	25,90 <sup>0</sup> S	28,22 <sup>0</sup> E	-	-	-	-	-	-	-	-	-	-	2	2	4

Furthermore, Figure 3.1.1 shows geographical positions of the stations in a more visible manner. As can be seen, the spatial coverage of the SHADOZ ozonesonde stations is also very irregular.

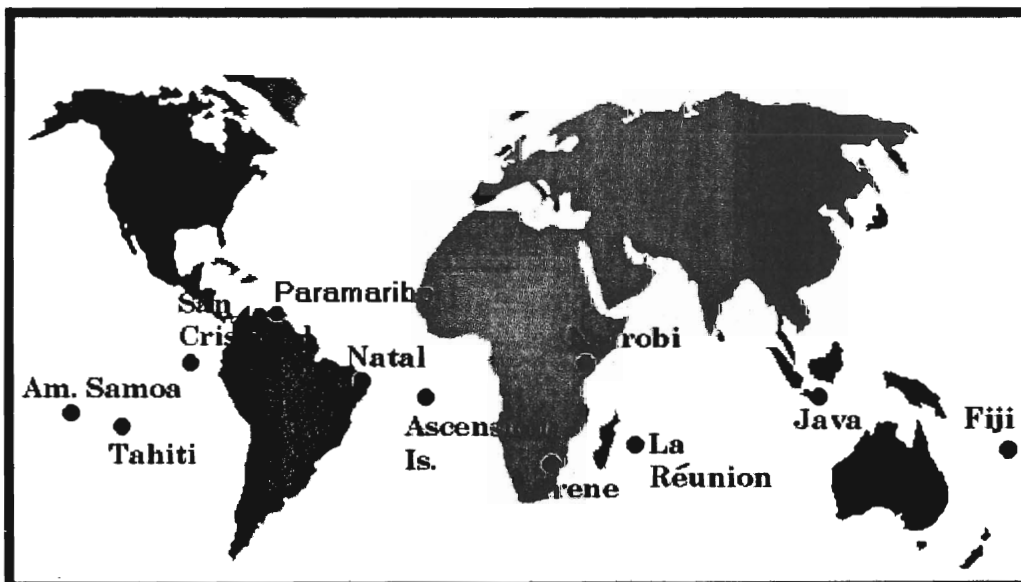


Figure 3.1.1 Overview of the geographical position of the SHADOZ ozonesonde stations. The Paramaribo station has also been depicted.

However, inspite of the fact that the used SHADOZ-data have a very irregular basis, a serious effort has been made to compare some observations with model calculations. Some considerations restricted our study to the ozonesonde stations in Ascension Island and Nairobi; since they have the greatest numbers of soundings during 1998 on a regular weekly basis, they are the stations best suited for a seasonality study. Also the ozonesonde station in San Cristobal will be subject of investigation; since in September 1998 five soundings were launched in ten days, these data are suitable to investigate the possibility of modelling daily changes in ozone profiles with TM3. Note that the aim of the study was only to evaluate the performance of the TM3 ozone simulations. Deficiencies found in the simulation can be due to a wide range of causes, which often fall outside the scope of this study.

## 3.2 Ascension Island

In this section the modeled ozone profiles of the station Ascension Island are compared with ozonesonde observations. The ozone soundings are detailed vertical measurements at one geographical position, which are difficult to compare to model calculations on a regular horizontal grid at fixed pressure levels. Such a comparison with individual soundings is also very sensitive to errors in the analyzed wind fields and to local emissions. Furthermore, the quality of a comparison of modeled and observed instantaneous ozone profiles would be rather poor in a statistical point of view, because regular ozone soundings are generally performed only once a week at most stations. In order to overcome the above mentioned difficulties, monthly averaged ozone values are considered. The modeled ozone profiles are then less dependent on the various simplifications which are present in the model, such as climatological emissions instead of emissions coupled to the actual meteorological parameters, prescribed deposition velocities regardless of the surface characteristics, and daytime averaged photolysis without a diurnal cycle [c.f. Wauben, 1998].

Since the ozonesonde station Ascension Island is located on an island far away from the continents, the observed ozone values should not be affected by local pollution. Let us first consider Figure 3.2.1, in which the monthly mean volume mixing ratios of ozone calculated by TM3 for February, May, August and November 1998<sup>i</sup> are presented together with all the observations in the corresponding months. All the observations are displayed in order to get an impression of the natural variability of observations.

---

<sup>i</sup> These months have been depicted in order to get isochroneous time-intervals.

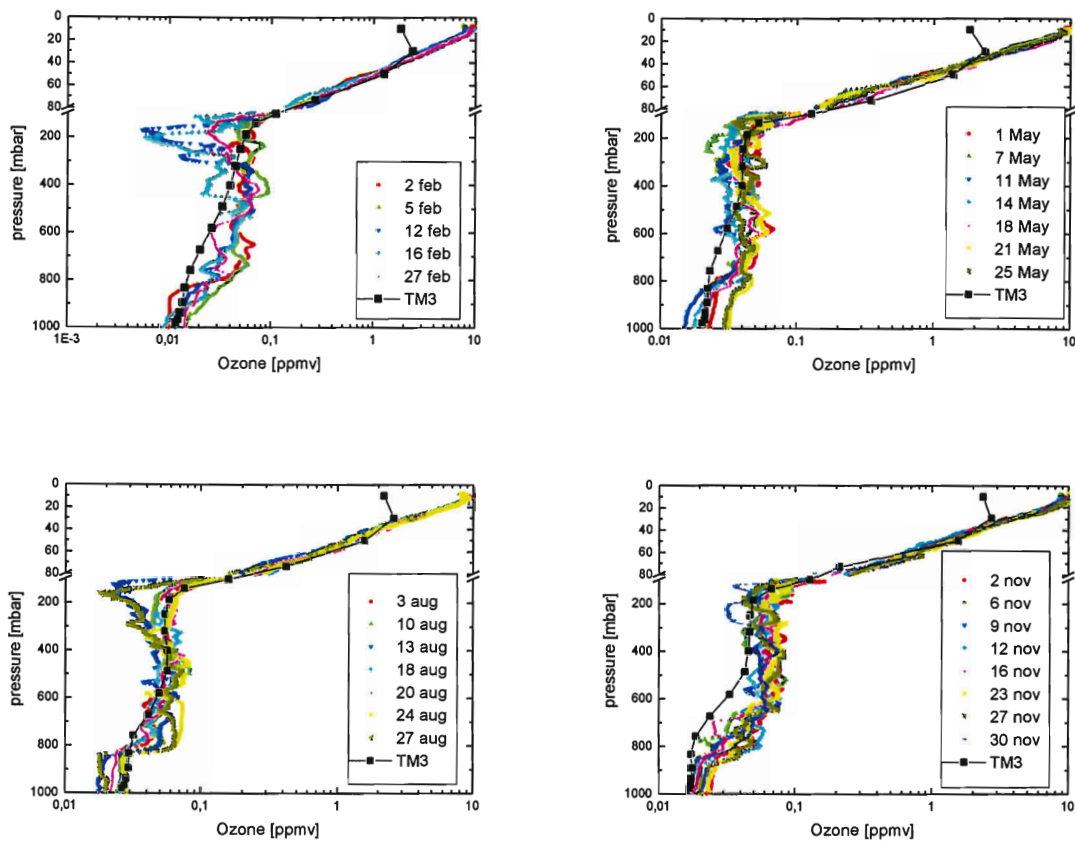


Figure 3.2.1 Monthly mean volume mixing ratios of ozone calculated by TM3 for February, May, August and November 1998 at Ascension Island together with the observations in the corresponding months.

As can be seen, the agreement between model results and observation is quite well, except for a deviation in the upper stratosphere (above 50 mbar). This deviation turns out to be a systematic deviation of the modeled ozone mixing ratio. Recall from chapter 2 that the chemical scheme of TM3 cannot adequately describe stratospheric chemistry and that therefore a zonally and monthly mean ozone climatology based on ozonesonde measurements [Fortuin and Langematz, 1995] is prescribed above 50 hPa. This is needed since the chemistry module in TM3 contains only relevant processes for the troposphere and lower stratosphere and as a result underestimates the amount of ozone formed under the influence of ultraviolet radiation higher in the stratosphere. Due to the low number of included observations from the tropics, this climatology could potentially be less reliable in the tropics.

The seasonality of the observed and modeled ozone values at Ascension Island is compared in Appendix A, Figure A.1. The monthly mean ozone values are given as a function of the month for all the nineteen standard vertical pressure levels in TM3 (i.e. 980, 967, 940, 895, 834, 758, 672, 582, 489, 402, 321, 250, 190, 140, 102, 73, 50, 30 and 10 mbar). All the observed ozone profiles from 1998 at Ascension Island have been interpolated to these vertical levels in order to get an

impression of the natural variability of observations. Note that, conform table 3.1.1, no observations are available for April.

Figure A.1 shows that in the upper stratosphere (i.e. 10, 30 and 50 mbar) is an evident systematic deviation of the modeled values in comparison with the observed values. It can be concluded that the prescribed climatology for the upper stratosphere in TM3 is less reliable for tropics, due to the low number of included observations in the tropics.

At levels in the lower stratosphere and upper troposphere (i.e. 73, 102, 140, 190, 250, 321 and 402 mbar) the modeled seasonality compares well with the observations, especially if one realises that no standard deviation bars are included in these plots. From other publications [e.g. Wauben, 1998] it can be seen that the standard deviation amounts to at least 5% for the simulated values.

Furthermore, at the lower levels (i.e. 489, 582, 672, 758, 834, 895, 940, 967 and 980 mbar) the modeled values compare reasonably well with the observed values. Only the values of the months September (9) and October (10) and November (11) show a small deviation. However, the seasonality of the ozone concentrations is still reproduced by TM3.

### **3.3 Nairobi**

In this section the modeled ozone profiles of the Nairobi station are compared with ozonesonde observations. In Figure 3.3.1, the monthly mean volume mixing ratios of ozone calculated by TM3 for January, May and September 1998 <sup>ii</sup> at Nairobi station, are presented together with all the observations in the corresponding months.

---

<sup>ii</sup> These months have been depicted in order to get isochroneous time-intervals.

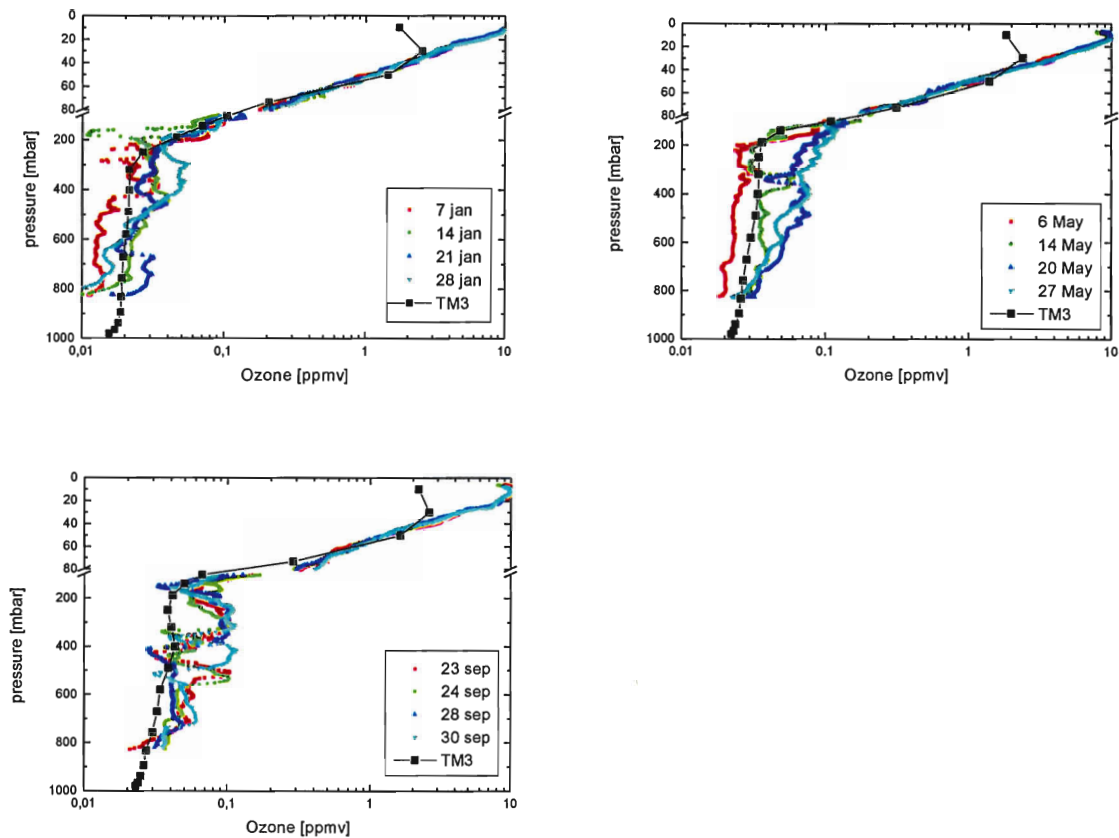


Figure 3.3.1 Monthly mean volume mixing ratios of ozone calculated by TM3 for January, May and September 1998 at Nairobi together with the observations in the corresponding months.

The agreement between model results and observation is quite well again, except for the systematic deviation in the upper stratosphere (above 50 mbar). Note also that the simulations sometimes show an underestimation in the troposphere.

Next the seasonality of the observed and modeled ozone values at Nairobi station will be compared. In Appendix B, Figure B.1, the monthly mean ozone values are given as a function of the month for the upper fourteen standard vertical pressure levels in TM3 (i.e. 758, 672, 582, 489, 402, 321, 250, 190, 140, 102, 73, 50, 30 and 10 mbar); there were no observations available of the lowest five levels (i.e. 980, 967, 940, 895 and 834 mbar). Again, the observed ozone profiles have been interpolated to these vertical levels in order to get an impression of the natural variability of observations. This time, no observations are available for July and August, conform table 3.1.1.

The levels in the (lower) troposphere (i.e. 489, 582, 672 and 758 mbar) show good results: the seasonality of the observed ozone concentrations is reproduced quite well by TM3. Higher up (> 402 mbar) the simulation gets worse and at levels in the upper stratosphere (i.e. 10, 30 and 50 mbar) a clear deviation is visible, with the same explanation (prescribed climatology is less reliable for the tropics) as before.



### 3.4 San Cristobal

Finally, modeled ozone profiles of September 1998 from the station San Cristobal are compared with ozonesonde observations. In Figure 3.4.1, all the ozonesonde measurements taken in september 1998 at San Cristobal station are displayed. Also the modeled monthly averaged ozone profile is displayed.

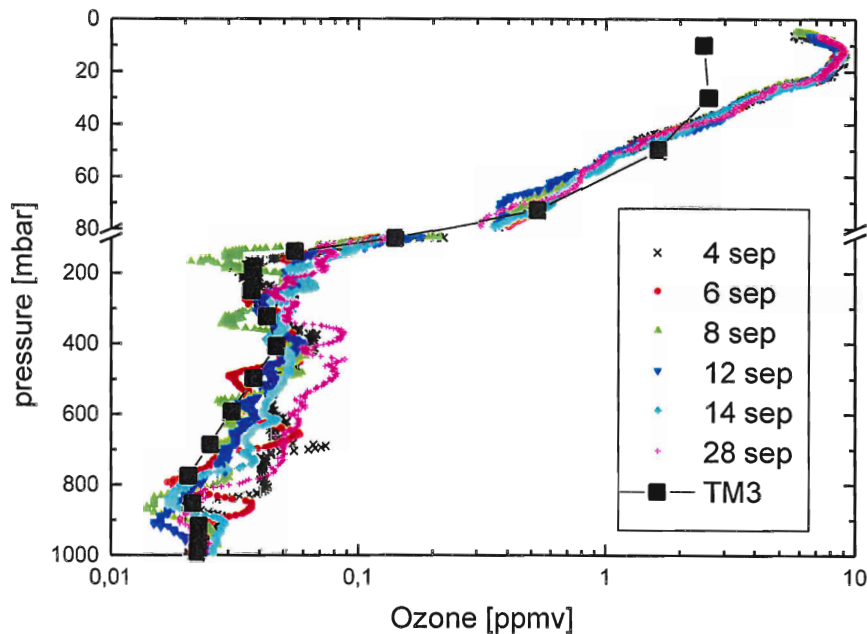


Figure 3.4.1 All observed instantaneous ozone profiles at San Cristobal and monthly mean ozone profile for September 1998 in ppmv.

As can be seen, the monthly mean model values are within the natural variability band defined by the instantaneous observations, except for the upper stratosphere (above 50 mbar).

Finally, an attempt has been made to reproduce individual soundings in September 1998 at the San Cristobal station, in order to investigate if it is possible to reproduce daily variability in ozone profiles with TM3. For this purpose, some subroutines, that produce ozone profiles at specific moments in time coinciding with the time of sounding (see appendix C), have been written and included in the TM3 model code. The results for these specific days in September 1998 are shown in Figure 3.4.2.

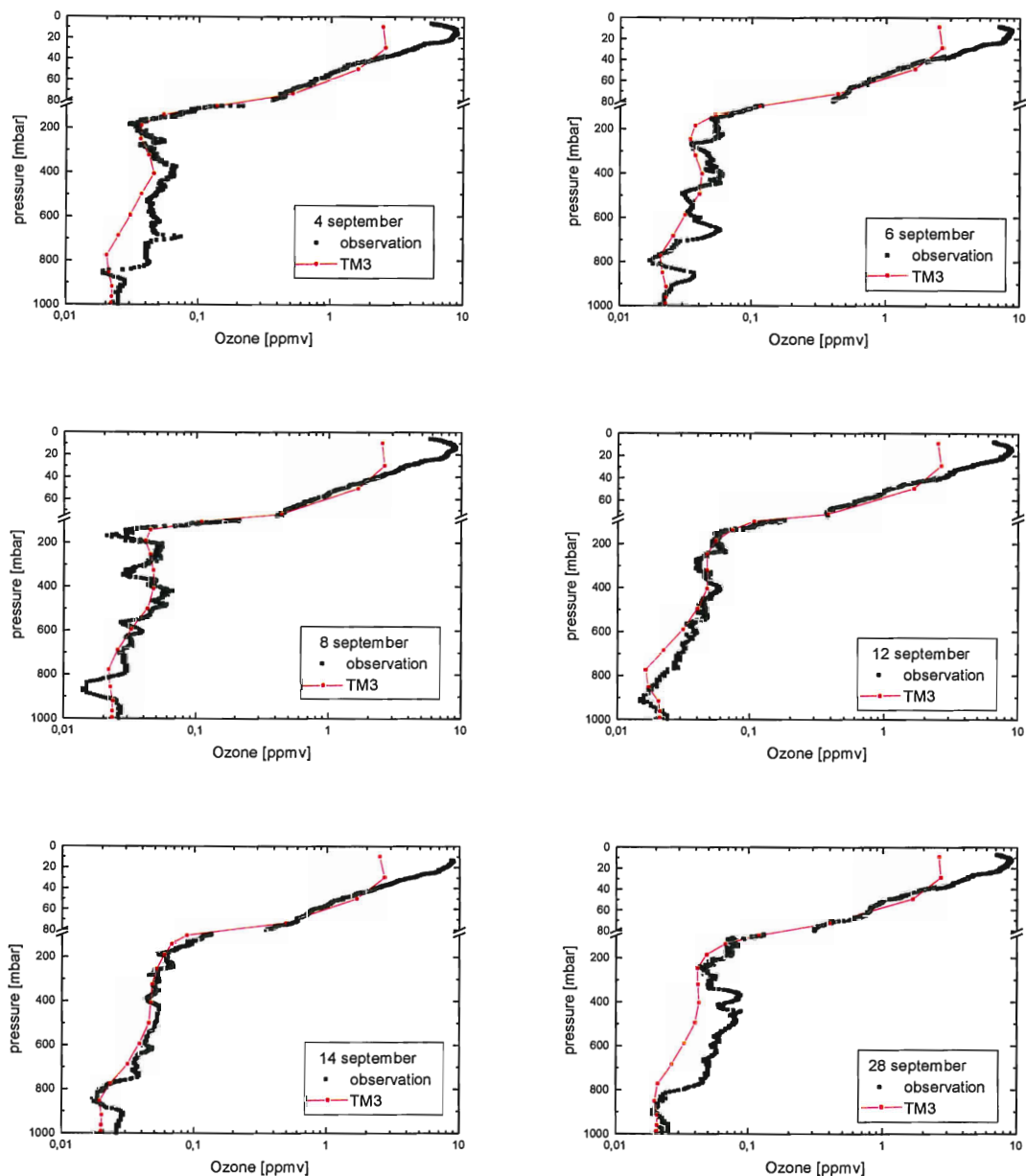


Figure 3.4.2 Observed and modeled instantaneous ozone profiles in ppmv at San Cristobal station at several days in September 1998.

At first sight the modeled profiles seem to compare reasonably well with observed profiles, except for the upper stratosphere. However, closer inspection clearly shows that the modeled ozone profiles cannot reproduce detailed features - like waves, advection of different sources and biomass burning - and that the simulations sometimes (e.g. 4 and 28 September) show an underestimation in the troposphere. The former deficiency is likely to be due to the limited resolution of TM3 ( $8^{\circ} \times 10^{\circ} \times 19$  vertical levels), the latter can be associated with imperfect chemistry, transport and sources/sinks.

## 4 Conclusions

Observed ozonesonde profiles in the tropics are compared with ozone distributions simulated by TM3 in order to validate the model results for ozone. The aim of the study was to evaluate the performance of the TM3 ozone simulations. Deficiencies found in these simulations can be due to a wide range of causes, which often fall outside the scope of this study.

TM3 uses meteorological data from ECMWF analyses for transporting the chemical constituents in combination with an ozone chemistry module containing methane and carbon monoxide oxidation chemistry. Also several emissions (e.g. NO<sub>x</sub>, CH<sub>4</sub>, and CO-emissions) are included. The ozone concentrations above 50 mbar are prescribed according to a zonally and monthly mean ozone climatology based on sonde measurement values.

The study was limited to three ozonesonde stations: Ascension Island, Nairobi and San Cristobal. Generally, monthly mean modeled ozone profiles compare reasonably well for all three stations with the natural variability constructed from all the available observations in the corresponding months, except for the upper stratosphere (above 50 mbar). In the upper stratosphere, an evident systematic deviation is visible. From this, it can be concluded that the prescribed climatology for the upper stratosphere in TM3 is less reliable for the tropics, due to the low number of included observations in the tropics.

Furthermore, the seasonality of ozone for the ozonesonde stations Ascension Island and Nairobi has been investigated. For Ascension Island, which is located on an island far away from the continents and which therefore should not be affected by local pollution, the seasonality is reproduced quite well by TM3, except for – again – the upper stratosphere. For Nairobi, which is located at the equatorial East-coast of Afrika, the seasonality is only reproduced reasonably well in the lower troposphere.

Finally, an attempt has been made to investigate the possibility to reproduce daily changes in ozone profiles with TM3. For this, individual soundings in September 1998 at the San Cristobal station were simulated. The conclusion is that the modeled ozone profiles are not accurate or sensitive enough to show detailed features, like waves, advection of different sources and biomass burning. Probably this can be explained by the very high spatial and temporal resolution required to reproduce these fine structures. The used model resolution of 8° x 10° x 19 vertical layers is probably not fine enough.

## 5 Epilogue and Acknowledgements

This report is a result of my traineeship at the KNMI (Royal Netherlands Meteorological Institute) in De Bilt. This report restricts to the comparison between observed ozonesonde profiles in the tropics with TM3 modeled ozone distributions. However, my traineeship has turned out to be much more comprehensive and diverse. Therefore, in Appendix D a schematic overview of all my activities has been added to this report.

Finally, I have come to the very pleasant task of expressing my gratitude to the people who have helped me to make my traineeship a succesfull and unforgettable one. Firstly, I like to thank my daily coaches Paul Fortuin and Peter van Velthoven and my supervisor prof. Kelder for their support and practical help. Next, I like to thank the many colleagues at KNMI, who gave me advice, information, and their time. Perhaps I might mention a few by name: Ernst Meijer, Rinus Scheele, Michiel van Weele and Hans Theihzen. Furthermore, I like to thank Cor Becker from the MDS (Meteorologische Dienst Suriname) for our constructive discussions. And last but not least, my appreciation goes to Jan Quik (and his family) and Bing Tan from the Anton de Kom University of Surinam. Besides the perfect working environment they provided me with, they showed me how beautiful, exciting and educational a country completely different from ours can be!

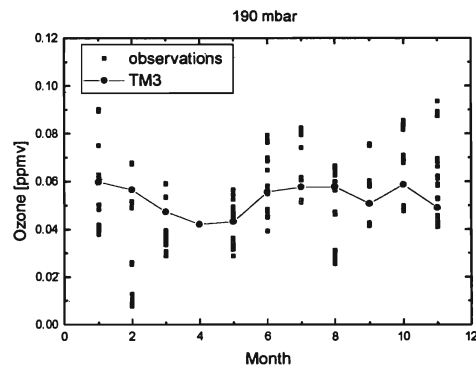
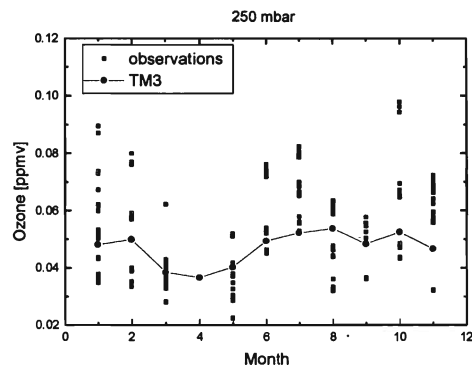
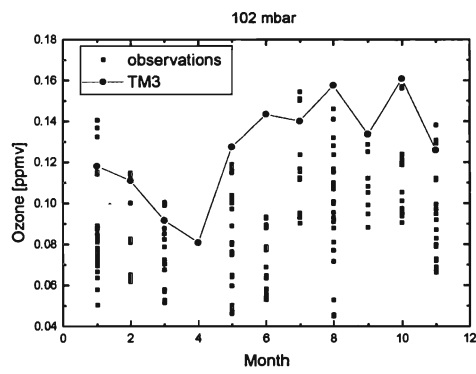
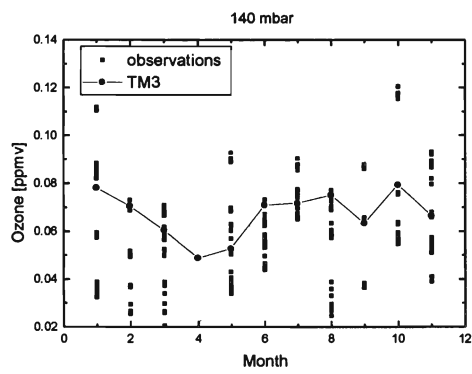
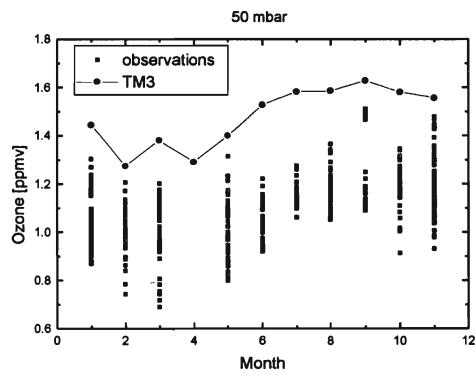
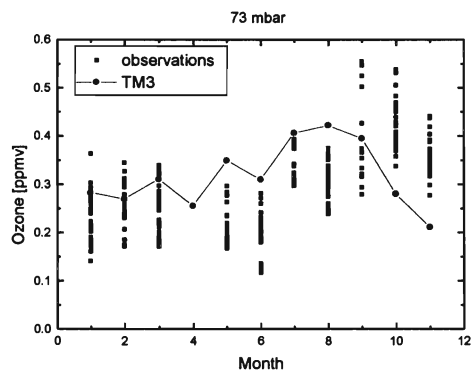
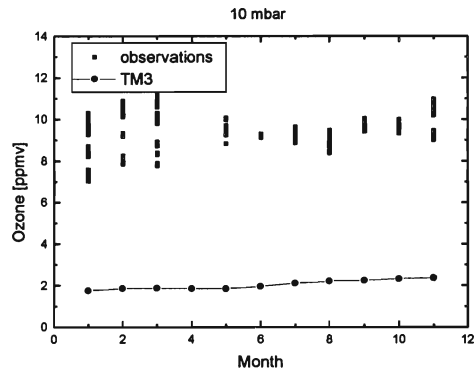
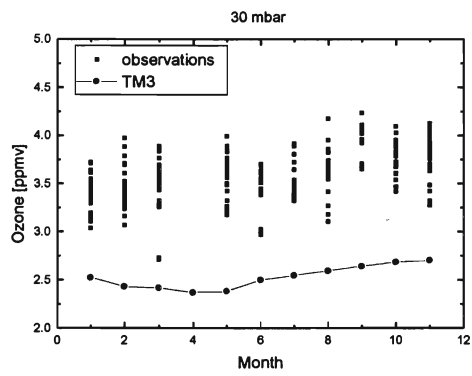
## 6 References

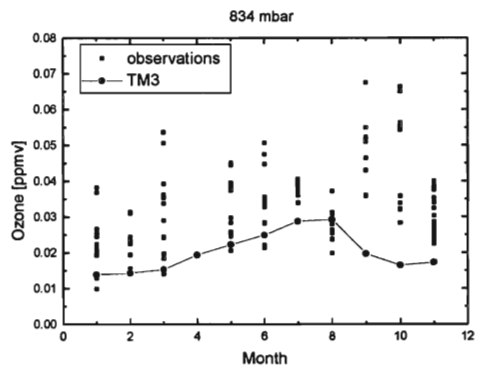
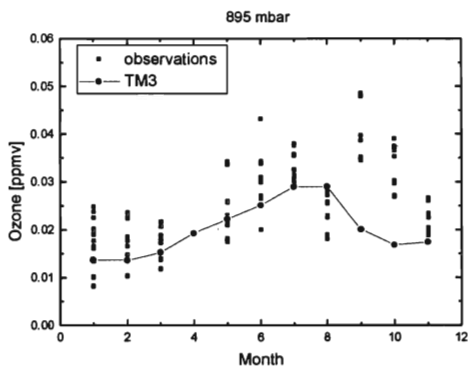
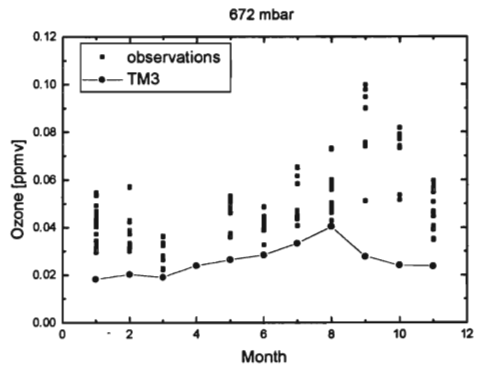
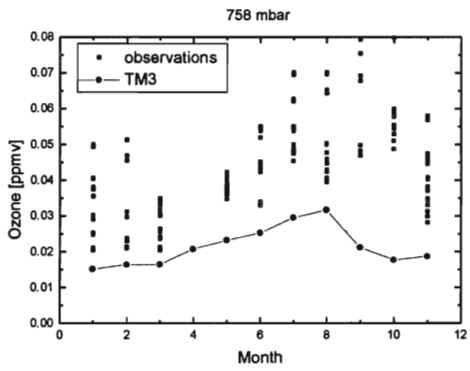
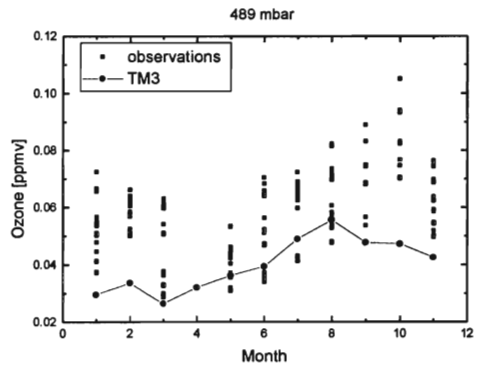
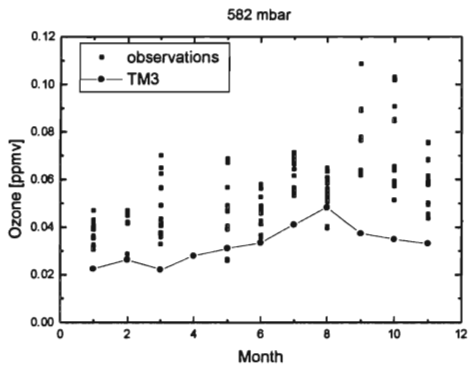
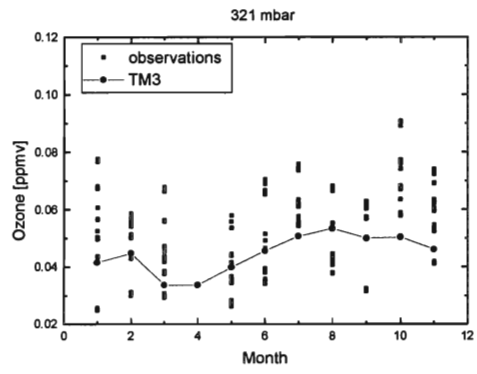
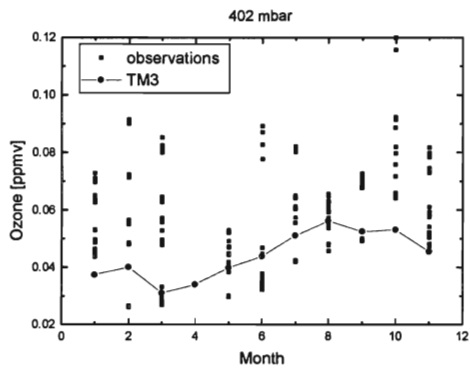
- AERONOX: "The Impact of NO<sub>x</sub> Emissions from Aircraft upon the Atmosphere at Flight Altitudes 8-15km" *Report of Sub-Project 3 on Global Atmosphere Model Simulations*, EU Project, (1995)
- Arpe, K., The hydrological cycle in the ECMWF short range forecasts, *Dynamics of Atmospheres and Oceans*, 16, 33-59, 1991.
- Atkinson, R., D.L. Baulch, R.A. Cox, R.F. Hampson, J.A. Kerr and J. Troe: "Evaluated Kinetic and Photochemical Data for Atmospheric Chemistry Supplement IV" *J. Phys. Chem. Ref. Data* 21, 1125-1568, 1992.
- Bruhl, C. and P.J. Crutzen: "On the Disproportionate role of Tropospheric Ozone as a Filter against Solar UV-B Radiation" *Geophys. Res. Letter*, 16, 703-706 (1989).
- Bruhl, C. and P.J. Crutzen: 1993, MPIC Two-Dimensional Model, in *The Atmospheric Effects of Stratospheric Aircraft: Report of the 1992 Models and Measurements Workshop*, edited by M.J. Prather and E.E. Remsburg, pp. 103-104 NASA Reference Publication 1292, vol. I, 1993.
- Crutzen, P.J. and P.H. Zimmermann, The changing photochemistry of the troposphere, *Tellus*, 43A B, 136-151, 1991.
- Crutzen, P.J., Ozone in the troposphere, *Composition, Chemistry, and Climate of the Atmosphere*, H.B. Singh (ED.), von Nostrand Reinhold Publ., 1995.
- DeMore, W.B., S.P. Sander, D.M. Golden, R.F. Hampson, M.J. Kurylo, C.J. Howard, A.R. Ravishankara, C.E. Kolb, and M.J. Molina, Chemical Kinetics and Photochemical Data for Use in Stratospheric Modeling - Evaluation Number 10, *JPL Publication 92-20*, Pasadena, California, USA, 1992.
- Dentener, F. and P.J. Crutzen, Reaction of N<sub>2</sub>O<sub>5</sub> on Tropospheric Aerosols: Impact on the Global Distributions of NO<sub>x</sub>, O<sub>3</sub>, and OH, *Journal of Geophysical Research*, 98D, 7149-7163, 1993.
- Dentener, F., Heterogenous Chemistry in the Troposphere, *PhD thesis, Faculteit Natuur-en Sterrenkunde, Universiteit Utrecht*, Utrecht, The Netherlands, 1993.
- Dianov-Klokov, V.I., and L.N. Yurganov, A Spectroscopic Study of the Global Space-time Distribution of Atmospheric Carbon Monoxide, *Tellus*, 33, 262-273, 1981.
- Dianov-Klokov, V.I., L.N. Yurganov, E.I. Grecho, and A.V. Dzhola, Spectroscopic Measurements of Atmospheric Carbon Monoxide and Methane. 1: Latitudinal Distribution, *Journal of Atmospheric Chemistry*, 8, 139-151, 1989.
- Fortuin, J.P. and U. Langematz, An update on the global ozone climatology and on concurrent ozone and temperature trends, in *Atmospheric Sensing and Modelling*, edited by R.P. Santer, Proceedings EUROPTO Series, 2311, pp.207-216, 1994.
- Fung, I., J. John, J. Lerner, E. Matthews, M. Prather, L.P. Steele and P.J. Fraser: Three Dimensional Model Synthesis of the Global Methane Cycle, *J. Geophys. Res.* 96, 13003-13065, 1991.
- Gardner, R.M., K. Adams, T. Cook, f. Deidewig, S. Ernedal, R. Falk, E. Fleuti, E. Hermse, C.E. Johnson, M. Lecht, D.S. Lee,, M. Leech, D. Lister, B. Masse, M. Metcalfe, P. Newton, A. Schmitt, C. vandenberh, R. van Drimmelen, The ANCAT/EC global inventory of NO<sub>x</sub> emissions from aircraft, *Atmos. Environ* 12, 1751-1766, 1997
- Heimann, M., The Global Atmospheric Tracer Model TM2, *Technical Report No.10*, Deutsches Kli-marechenzentrum, Hamburg, Germany, 1995.
- Hein, R., Inverse Modellierung des atmosphärischen Methan-Kreislaufs unter Verwendung eines drei dimensional Modells des Transports und der Chemie der Troposphäre, *PhD thesis, Fachbereich Geowissenschaften der Universität Hamburg*, Hamburg, Germany, 1994.
- Hein, R. and M. Heimann, Determination of Global Scale Emissions of Atmospheric

- Methane Using An Inverse Modelling Method, in *Non- CO<sub>2</sub> Greenhouse Gases*, edited by J. van Ham *et al.*, pp. 271-281, Kluwer Academic Publishers, Dordrecht, The Netherlands, 1993.
- Hein, R., P.J. Crutzen, and M. Heimann, An Inverse Modeling Approach to Investigate The Global Atmospheric Methane Cycle, *Global Biogeochemical Cycles*, submitted, 1996
- Holton, J.R., On the Global Exchange of Mass between the Stratosphere and Troposphere, *J. Atmos. Sci.* **47**, 392-395, 1990.
- Junge, C.E. and P.E. Gustafson, On the distribution of sea salt over the United States and its removal by precipitation, *Tellus*, **9**, 164-173, 1957.
- Louis, J.F., A parametric model of vertical eddy fluxes in the atmosphere. *Boundary Layer Meteorology*, **17**, 6579-6613, 1979.
- Meijer, E.W., P.F.J. van Velthoven, A.M. Thompson, L. Pfister, H. Schlager, P. Schulte and H. Kelder: Model calculations of the impact of NO<sub>x</sub> from air traffic, lightning, and surface emissions, compared with measurements. *J. Geophys. Res.* **105**, 3833-3850, 2000
- Newell, R.W., J.W. Kidson, D.G. Vincent, and G.J. Boer, The general circulation of the tropical atmosphere and interactions with extratropical latitudes, *MIT Press*, **2**, Cambridge, Mass., 1974.
- Price, C. and D. Rind, Modeling Global Lightning Distributions in a General Circulation Model, *Monthly Weather Review*, **122**, 1930-1937, 1994.
- Russell, G.L. and J.A. Lerner, A new finite-differencing scheme for the tracer transport equation, *Journal of Applied Meteorology*, **20**, 1483-1498, 1981.
- Tiedtke, M., A Comprehensive Mass Flux Scheme for Cumulus Parametrization in Large-Scale Models, *Monthly Weather Review*, **117**; 1779-1800, 1987.
- Thompson, A. M. and Witte J. C., A new data set for the Earth Science Community, *Earth Observer*, **11**(4), 27-30, 1999. SHADOZ website:  
[http://hyperion.gsfc.nasa.gov/Data\\_services/shadoz/Shadoz\\_hmpg2.html](http://hyperion.gsfc.nasa.gov/Data_services/shadoz/Shadoz_hmpg2.html)
- Velders G.J.M., Heijboer L.C. and Kelder H., The simulation of the transport of aircraft emissions by a three-dimensional global model, *Ann. Geophys.* **12**, 385-393, 1994.
- Wauben, W.M.F., J.P.F. Fortuin, P.F.J. van Velthoven, H.M. Kelder, Comparison of modeled ozone distributions with sonde and satellite observations, *Journal of Geophysical Research*, Vol.103, No D3, Pages 3511-3530, 1998
- Wauben, W.M.F., P.F.J. van Velthoven, H. Kelder, Changes in tropospheric NO<sub>x</sub> and O<sub>3</sub> due to subsonic aircraft emissions, KNMI Scientific Report; WR 95-04, 1995.

# Appendix A

## Ascension Island







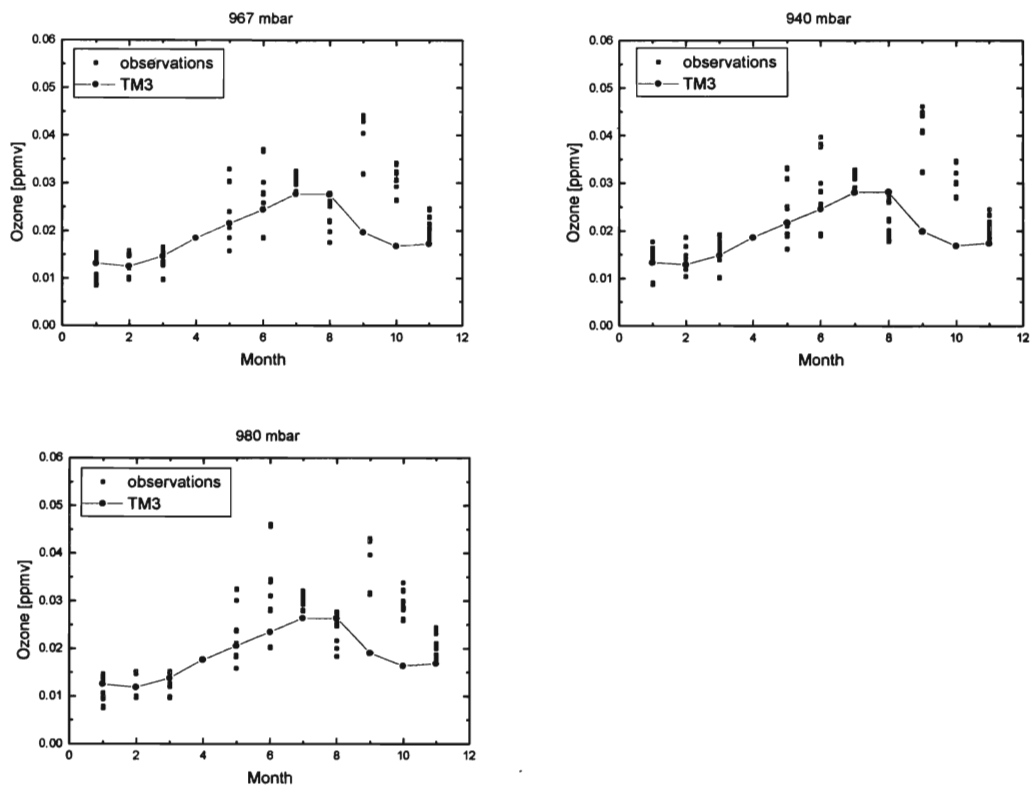
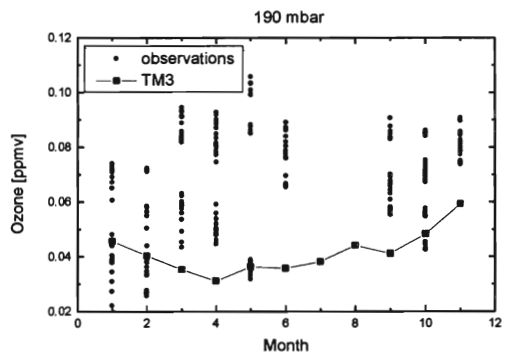
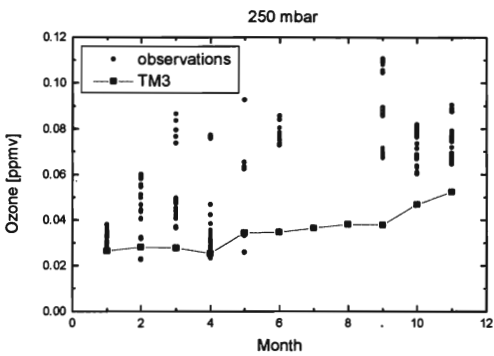
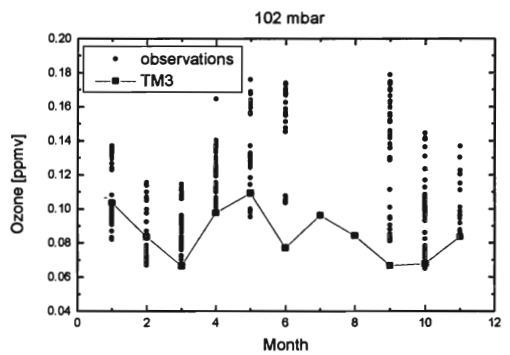
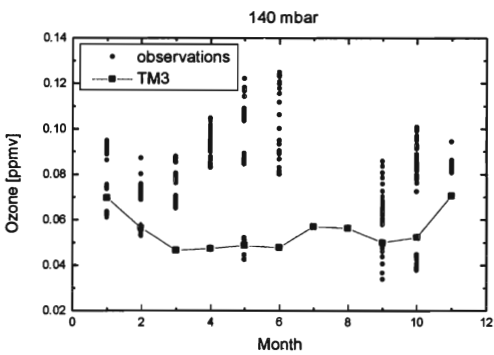
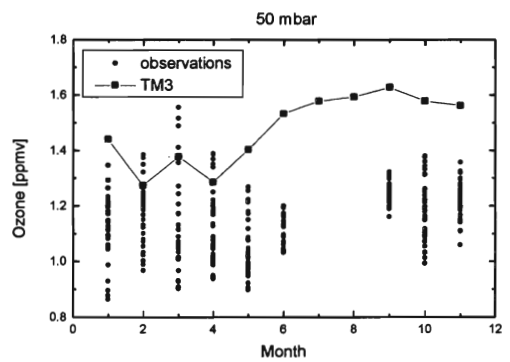
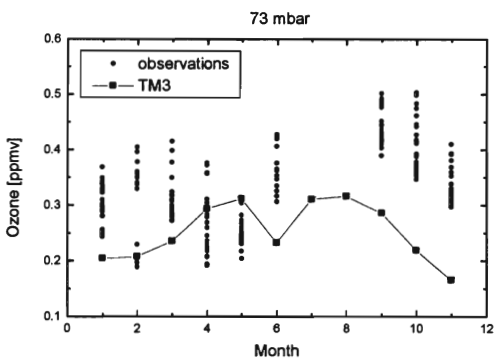
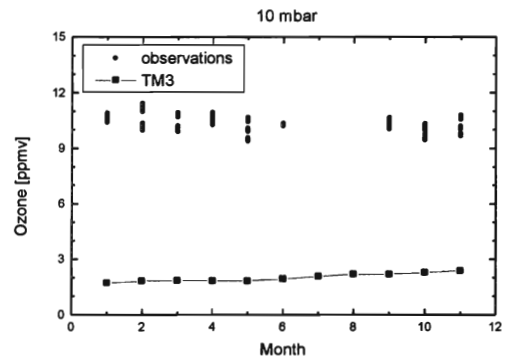
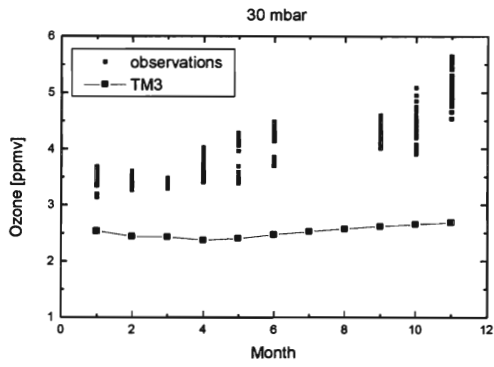


Figure A.1 The seasonality of observed and modeled monthly mean ozone for Ascension Island station at standard vertical TM3-levels. By displaying all the observations during 1998, an impression of the natural variability is developed to compare with model calculations.

# Appendix B

## Nairobi



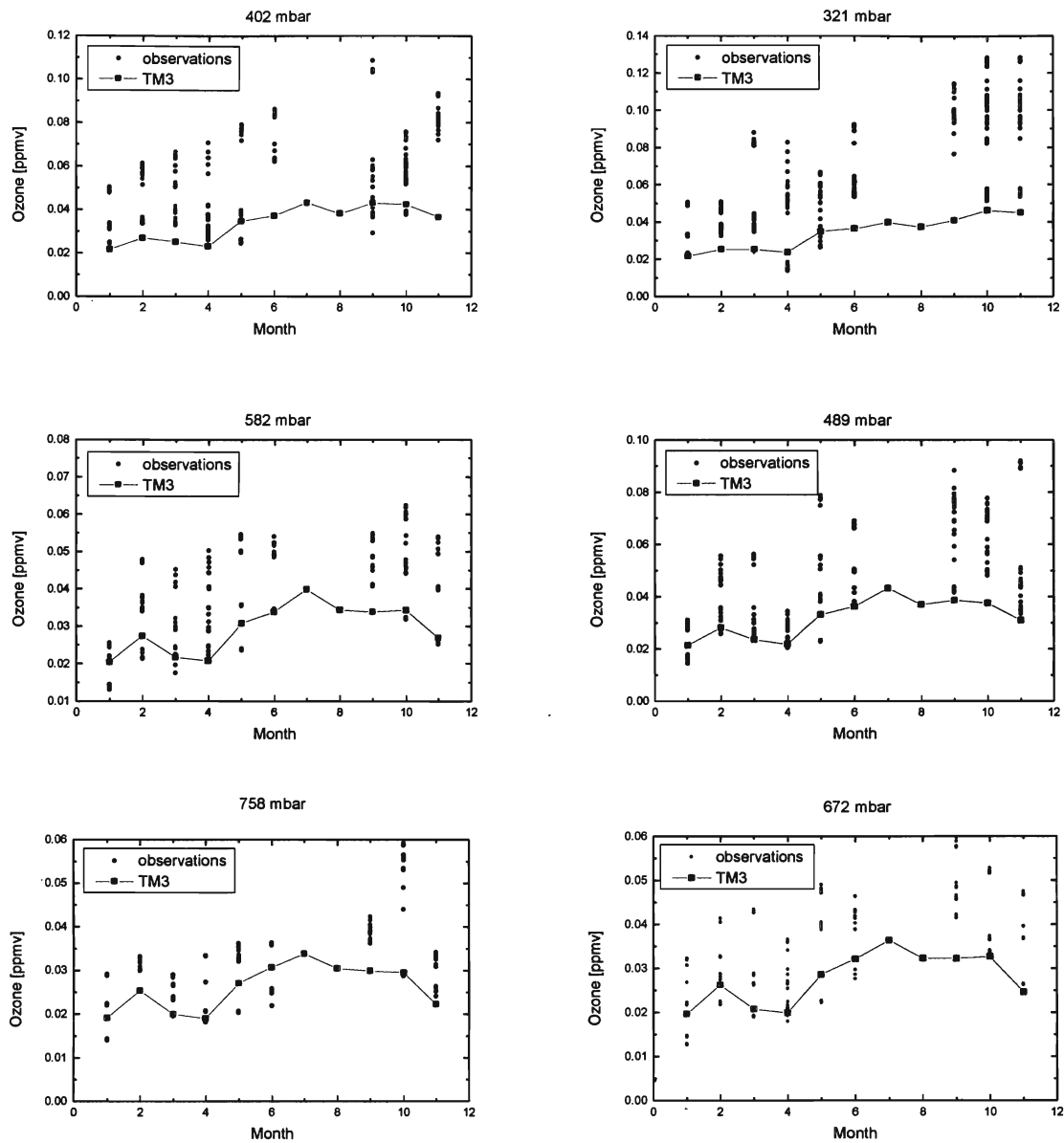


Figure B.1 The seasonality of observed and modeled monthly mean ozone for Nairobi station at standard vertical TM3-levels. By displaying all the observations during 1998, an impression of the natural variability is developed to compare with model calculations.

## Appendix C

In this Appendix the subroutines are displayed, that were written in order to produce ozone profiles at specific moments in time that coincide with the time of sounding.

```
      subroutine SOUNDING
c-----
c
c gives output at position of sounding, at midday
c
c output is date, lat, lon, p(hPa), T(K), O3(ppmv)
c
c called from : tracer
c               every nchem seconds !
c
c expected input file is "sounding.dat", containing date, lat, lon
c if "sounding.dat" does not exist, no output is generated.
c
c for each sounding a new output file is generated with the
c name: sound_yyyymmdd.d
c
c It is not possible to evaluate multiple soundings on 1 day!!!
c-----

      implicit none
      include "constants"
      include "common"

      external openfile, getsounding

      integer ksi,kso      ! input and output file unit numbers
      parameter(ksi=41,kso=42)
      character*16 fout    ! name of output file
      integer date,lat,lon ! date, and lat,lon position of sounding
      integer ix,iy       ! x,y indices of sounding's position
      integer iz          ! loop variable over column
      integer tm3date     ! idate converted to yyyymmdd format
      real loctime       ! local time at (lat,lon)
      real press         ! pressure (hPa)
      real temp          ! temperature (K)
      real o3            ! [O3] (ppmv)
      logical fex        ! flag for existing of sounding.dat
      logical first      ! flag for initializing routine
      data first /.true./

      save first,fex,fout,date,ix,iy,lat,lon

c INITIALISATION

      if (first) then
         first = .false.
         inquire (file='sounding.dat',exist=fex)
         if (fex) then
            open (unit=ksi,file='sounding.dat',status='old')
            read (ksi,*)
            call GETSOUNDING(fex,ksi,date,lat,lon,ix,iy)

```

```

        read (ksi,*) date,lat,lon
        call OPENFILE(kso,fout,date)
    endif
endif

if (.not.fex) return          ! no sounding data

C
C GIVE OUTPUT AT REQUESTED DATA AT (AS CLOSE AS POSSIBLE TO) MIDDAY
C
tm3date = idate(3)+100*(idate(2)+100*idate(1))
loctime = mod(float(idate(4))+24.*float(ix-1)/float(im)+12.,24.)

if (tm3date.eq.date.and.abs(loctime-12.) .le.nchem) then

    do iz=1,lm
        temp = t(ix,iy,iz)
        press= (phlb(ix,iy,iz)+phlb(ix,iy,iz+1))/2.
        o3   = 1.e6 * rm(ix,iy,iz,iO3) / ra(iO3) * m(ix,iy,iz)
        write(kso,'(i10,4f7.2,1p,e11.3)') date,lat,lon,press,temp,o3
    enddo
    close(kso)
    call GETSOUNDING(fex,ksi,date,lat,lon,ix,iy)
    if (fex) call OPENFILE(kso,fout,date)
endif

return
end

```

**subroutine OPENFILE(kso,fout,date)**

```

C-----
C
C opens outputfile for each new sounding
C
C-----

```

```

implicit none
include 'constants'
include 'common'
character*16 fout

integer      kso,date
write(fout,'(a6,i8,a2)') 'sound_',date,'.d'
open (unit=kso,file=fout,status='new')
write(kso,'(a10,4a7,a11)') 'date', 'lat', 'lon', 'p(hPa)',
$                          'T(K)', 'O3(hPa)'

return
end

```

**subroutine GETSOUNDING(fex,ksi,date,lat,lon,ix,iy)**

```

C-----
C
C get new sounding data: date and x,y position
C
C-----

```

```

implicit none
include 'constants'
include 'common'

```

```
logical fex
integer ksi,date,ix,iy,lat,lon
integer tm3date

date = -999
tm3date = idate(3)+100.*(idate(2)+100.*idate(1))
do while (date.lt.tm3date)
  read (ksi,*,end=9999) date,lat,lon
enddo
ix = int((lon+180.)*float(im)/360.)+1
iy = int((lat+ 90.)*float(jm)/180.)+1
return
9999 continue      ! get here if no more sounding data is available
fex=.false.

return
end
```

## Appendix D

A schematic overview of all my activities during my traineeship at KNMI.

Weeknumber	Place	Activities
1	KNMI, De Bilt	Introduction into the field of research by reading several (TM3 related) articles and articles about climatology in the tropics.
2	KNMI, De Bilt	Introduction into some elementary UNIX and elementary Fortran by reading and "playing" with the computer.
3	KNMI, De Bilt	Finding out how TM3 works by reading an obsolete manual and "playing" with the computer.
4	KNMI, De Bilt	More finding out how TM3 works by reading an obsolete manual and "playing" with the computer and performing some TM3 runs.
5	KNMI, De Bilt	Performing more TM3 runs and evaluating of the obtained TM3 results.
6 & 7	KNMI, De Bilt	Translation of the UNIX based version of TM3 into a LINUX based PC version. In practise this implied installing LINUX on a PC, compiling the Fortran code again with a Fortran PGF90 compiler and rewriting the binary input files.
8	KNMI, De Bilt	Testing the LINUX based PC version of TM3 and studying the working principles of a photometric ozone analyser and following a short course into installing this ozone analyser.
9	Anton de Kom University, Paramaribo	Installing a dual bootable system (LINUX & Windows) at a PC and installing and testing TM3.
10	Anton de Kom University, Paramaribo	Due to a Harddisk error, TM3 had to be re-installed several times.
11	Anton de Kom University, Paramaribo	Writing a step-by-step "TM3 installation procedure" for possible TM3 users and controlling this procedure by having TM3 installed on a PC by a potential user.
12	Anton de Kom University, Paramaribo	Writing a completely up-to-date "Model documentation" for potential users. This report can also be very usefull for new TM3-users at KNMI, since a proper documentation is not present.
13	Anton de Kom University, Paramaribo	Finishing the "Model documentation" and showing some TM3 demonstrations.
14	Anton de Kom University, Paramaribo	Preparation of a 50 minutes guest-course about "Modelling in Atmospheric Research" and keeping the guest-course. Showing some more TM3 demonstrations.
15	Meteorological Service Surinam (MDS), Paramaribo	Writing a step-by-step procedure to install the ozone-analyser , since the ozone-analyser didn't arrive.
16, 17 & 18	KNMI, De Bilt	Further investigation of TM3 results and writing this final report.





## OVERZICHT VAN KNMI-PUBLICATIES, VERSCHENEN SEDERT 1999

### KNMI-PUBLICATIE MET NUMMER

- 186-II Rainfall generator for the Rhine Basin: multi-site generation of weather variables by nearest-neighbour resampling / T. Brandsma a.o.
- 186-III Rainfall generator for the Rhine Basin: nearest-neighbour resampling of daily circulation indices and conditional generation of weather variables / Jules J. Beersma and T. Adri Buishand
- 186-IV Rainfall generator for the Rhine Basin: multi-site generation of weather variables for the entire drainage area / Rafal Wójcik, Jules J. Beersma and T. Adri Buishand
- 188 SODA workshop on chemical data assimilation: proceedings; 9-10 December 1998, KNMI, De Bilt, The Netherlands
- 189 Aardbevingen in Noord-Nederland in 1998: met overzichten over de periode 1986-1998 / [Afdeling SO]
- 190 Seismisch netwerk Noord-Nederland / [afdeling Seismologie]
- 191 Het KNMI-programma HISKLIM (HIStorisch KLIMAat) / Theo Brandsma, Frits Koek, Hendrik Wallbrink, Günther Können
- 192 Gang van zaken 1940-48 rond de 20.000 zoekgeraakte scheepsjournalen / Hendrik Wallbrink en Frits Koek

### TECHNISCH RAPPORT = TECHNICAL REPORT (TR)

- 216 Evaluatierapport Automatisering Visuele Waarnemingen : Ontwikkeling Meestsystemen / Wiel Wauben en Hans de Jongh
- 217 Verificatie TAF en TREND / Hans van Bruggen
- 218 LEO - LSG and ECBILT coupled through OASIS: description and manual / A. Sterl
- 219 De invloed van de grondwaterstand, wind, temperatuur en dauwpunt op de vorming van stralingsmist: een kwantitatieve benadering / Jan Terpstra
- 220 Back-up modellering van windmeetmasten op luchthavens / Ilja Smits
- 221 PV-mixing around the tropopause in an extratropical cyclone / M. Sigmond
- 222 NPK-TIG oefendag 16 december 1998 / G.T. Geertsema, H. van Dorp e.a.
- 223 Golfhoogteverwachtingen voor de Zuidelijke Noordzee: een korte vergelijking van het ECMWF-golfmodel (EPS en operationeel), de nautische gidsverwachting, Nedwam en meteoroloog / D.H.P. Vogelesang, C.J. Kok
- 224 HDFg library and some HDF utilities: an extension to the NCSA HDF library user's manual & reference guide / Han The
- 225 The Deelen Infrasound Array: on the detection and identification of infrasound / L.G. Evers and H.W. Haak
- 226 2D Variational Ambiguity Removal / J.C.W. de Vries and A.C.M. Stoffelen
- 227 Seismo-akoestische analyse van de explosies bij S.E. Fireworks ; Enschede 13 mei 2000 / L.G. Evers en H.W. Haak
- 228 Evaluation of modified soil parameterization in the ECMWF landsurface scheme / R.J.M. Ijpelaar
- 229 Evaluation of humidity and temperature measurements of Vaisala's HMP243 plus PT100 with two reference psychrometers / E.M.J. Meijer
- 230 KNMI contribution to the European project WRINCLE: downscaling relationships for precipitation for several European sites / B.-R. Beckmann and T.A. Buishand
- 231 The Conveyor Belt in the OCCAM model: tracing water masses by a Lagrangian methodology / Trémeur Balbous and Sybren Drijfhout
- 232 Analysis of the Rijkooit-Weibull model / Ilja Smits

### WETENSCHAPPELIJK RAPPORT = SCIENTIFIC REPORT (WR)

- 99-01 Enhancement of solar and ultraviolet surface irradiance under partial cloudy conditions / Serdal Tunç
- 99-02 Turbulent air flow over sea waves: simplified model for applications / V.N. Kudryavtsev, V.K. Makin and J.F. Meirink
- 99-03 The KNMI Garderen experiment, micro-meteorological observations 1988-89: corrections / Fred C. Bosveld
- 99-04 ASGAMAGE: the ASGASEX MAGE experiment : final report / ed. W.A.Oost
- 00-01 A model of wind transformation over water-land surfaces / V.N. Kudryavtsev, V.K. Makin, A.M.G. Klein Tank and J.W. Verkaik
- 00-02 On the air-sea coupling in the WAM wave model / D.F. Doortmont and V.K. Makin.
- 00-03 Salmon's Hamiltonian approach to balanced flow applied to a one-layer isentropic model of the atmosphere / W.T.M. Verkley
- 00-04 On the behaviour of a few popular verification scores in yes-no forecasting / C.J. Kok
- 01-01 Hail detection using single-polarization radar / Iwan Holleman
- 02-01 Comparison of modeled ozone distributions with ozonesonde observations in the tropics / Rob Puts





